SSRG International Journal of Mechanical Engineering
ISSN: 2348-8360/ https://doi.org/10.14445/23488360/IJME-V12I12P103

Volume 12 Issue 12, 19-30, December 2025

Original Article

Design and Fabrication of Omni Directional H-Bot and Determining Stability Using Edge Impulse Software

Rakesh Rajendran[1], Hamsadhwani Vivekanandhan[2], Shivakumar Natarajan[3], Karthick. M[4], Sharmila Begum. M[5], Sugavaneswaran. M[6]

[1]*Department of ECE, Periyar Maniammai Institute of Science and Technology, Thanjavur, Tamil Nadu, India.*
[2]*Department of EEE, Periyar Maniammai Institute of Science and Technology, Thanjavur, Tamil Nadu, India.*
[3]*Department of Mechanical Engineering, Periyar Maniammai Institute of Science and Technology, Thanjavur, Tamil Nadu, India.*
[4]*Department of Education, Periyar Maniammai Institute of Science and Technology, Thanjavur, Tamil Nadu, India.*
[5]*Department of CSE, Periyar Maniammai Institute of Science and Technology, Thanjavur, Tamil Nadu, India.*
[6]*Prag Robotics pvt ltd, Chennai, Tamilnadu, India.*

[1]*Corresponding Author : rak2win@gmail.com*

Received: 06 October 2025 Revised: 07 November 2025 Accepted: 08 December 2025 Published: 27 December 2025

Abstract *- Wall Climbing Robots (WCR) are emerging with drastic development, and their role has become inevitable across many industrial applications. The performance of these WCRs is directly influenced by their adhesive mechanism and its capability to travel in multiple directions. Though there are many research papers that have worked on wall climbing robots, only a few papers have focused on this multi-directional or omni directional wall climbing robot. In this paper, an innovative model is proposed with two linear actuators coupled with each other and having solenoids at both ends as the adhesive medium. It is also enabled with a central disc having three solenoids that enhance the omni direction rotation of the H-bot. The mathematical model for the proposed H-bot is obtained through a free-body diagram. FEMM software is used to visualize the magnetic field strength of the proposed design. The design is modelled with simulation software named Coppelia Sim and then tested with actual fabrication in the lab test. The time taken to climb the particular height, both in simulation testing and actual experimental testing, is compared and analyzed. An IoT software named Edge Impulse is used to study the stability of the proposed H-bot. This stability analysis is performed for both climbing and descending of the H-bot on a vertical wall. This stability analysis is also performed during the omni direction rotation when the solenoids in the central disc are energized.*

Keywords *- Edge impulse software, H-bot, Coppelia Sim, FEMM, Free body diagram.*

1. Introduction

The wall-climbing robots are mainly classified based on their locomotive and adhesive types. The most important constraint in the design of these wall-climbing robots is their ability to overcome the discontinuity on the wall and their ability to change the direction of navigation for the given adhesive mechanism that limits their payload capacity. There are many types of adhesive media applied, namely magnetic, suction or vacuum, electrochemical, rope and rail adhesive, etc. Author have compared the p: w value for the existing WCR. Similarly, the WCR are classified based on locomotive type as legged type, wheeled type, crawling type, and hybrid type. The performance of the bot varies based on the combination of these locomotive and adhesive types. In this paper, an innovative model is proposed in the form of an H-shape and hence named as 'H-bot' by considering a legged mechanism and a magnetic adhesive medium. The magnetic adhesive medium can be further classified based on whether it uses a permanent magnet or an electromagnet, as shown in Figure 1. Each mechanism is further classified based on its locomotive type. The proposed H-Bot has two linear actuators, which in turn have two solenoids each. The solenoids in the linear actuators are named as a1, a2, b1, and b2. Here, two linear actuators are coupled with a central electromagnetic disc having three solenoids named as c, d, and e. These central electromagnetic disc enables the rotation movement covering 360-degree coverage, enabling multi-directional access. There is a substantial amount of literature related to the magnetic and electromagnetic adhesive mechanism for wall-climbing robots, which has been utilized in the design of the proposed H-bot. Howlader et al [1] proposed a WCR using a magnetic adhesive method for performing NDT. He used the FEA method for analyzing the proposed design. Kalra et al [2] designed a permanent magnetic adhesive wall climbing robot. Lee et al [3] proposed a transition wall climbing robot capable of performing 90 ° and 240 ° wall-to-wall transitions. Huang et al [4] proposed a wall-climbing robot with magnets to climb ferromagnetic structures. Wang et al [5] proposed a high payload-to-weight ratio wheeled WCR.

Table 1. Comparison of features of existing research on magnetic wall climbing robot with features of proposed H bot wall climbing robot

Robot / Paper (Year)	Weight	Payload	Adhesive Force / Mechanism	Navigation / Direction Ability	Ability to handle discontinuity of wall
Magnetic Wheeled Robot – Design & Fabrication Using Magnetic Adhesion (2025) A. Khan et al. [13]	2.08 kg	1.56 kg	Permanent magnets (magnetic wheels; not force-quantified)	Vertical & inverted transitions (rocker-bogie mechanism)	Cannot navigate
NuBot: Magnetic Adhesion Robot – (2023, sprung passive suspension) H. Xu et al.[14]	~0.98 kg–1 kg* (approx.)	0.6–0.8 kg (varies by surface) max 3.6 kg	Permanent magnetic wheels; adhesive force distribution inferred experimentally	Unidirectional vertical & curved wall	Cannot navigate
Magnetic Crawler w/ Load Dispersion Mechanism – (2022 study) Hu et al [15]	74 kg	150 kg (static)	450 N per magnetic unit (18 units on wall stack)	unidirectional crawling on vertical & convex surfaces	Cannot navigate
Magnecko – Quadrupedal Magnetic Climbing Robot (2025) S. Leuthard et al. [16]	11.3 kg	≥ 65 % of own weight (approximately 7.3 kg)	Electro-Permanent Magnets (EPMs), robust adhesion for ferrous surfaces	Omni-directional locomotion including vertical, horizontal, overhang, concave corners	Can navigate
Bi-Wheeled WCR (BWWCR) – R. Rajendran et al [17]	≈1.7 kg	15kg	660 N total desired adhesive force (330 N per magnetic wheel made of NdFeB N55)	Omnidirectional (any direction on vertical + transitions)	Cannot navigate
Proposed H-Bot wall climbing robot	5 kg	70 kg (static) 18kg(dynamic)	1617 N (1029 from central disc used for direction change -static+588 N from 4 solenoids connected with linear actuators used for dynamic ie forward and backward navigation)	Omnidirectional (any direction on vertical and horizontal)	Can navigate

Jiang et al [6] designed a wall climbing robot using FEA analysis using ANSYS. Li et al [7] presented a bioinspired reversible adhesive WCR. Qian et al [8] developed WCR with chain feet negative pressure. Yang et al [9] presented WCR with the help of a simulation and surrogate model. He also analyzed the stability of the adhesion. Wang et al [10] introduced an ant overturning method mainly applied to overcome the obstacles. Author proposed a simulation model using Coppelia Sim to analyze payload capacity before fabrication.

Zhu et al [11] reviewed in detail the current advancement in the technology for wall-climbing robots. Author designed a WCR with a permanent magnet with an adjustable and non-contactable adhesive mechanism. Wu et al [12] presented a hybrid adhesive WCR with both magnet and electromagnet as adhesive material. In this paper, FEMM was used as an analysis software to determine the interference of magnetic flux lines of the proposed design. Detailed comparison is shown in Table 1.

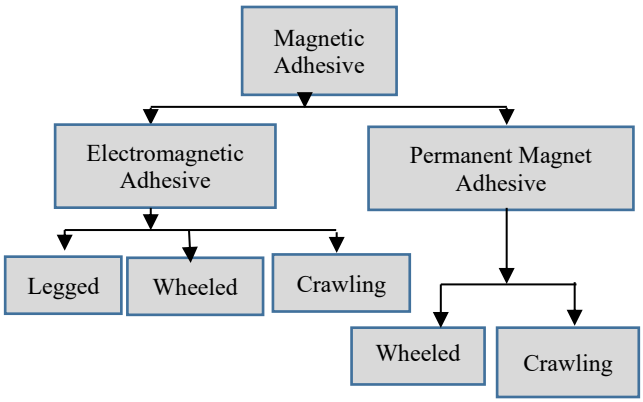

Fig. 1 Classification of magnetic adhesive type WCR

2. Simulation Design and Fabrication

The software, earlier named Vrep and currently known as Coppelia Sim, is used for modelling the proposed H-Bot. There are two prismatic joints used as linear actuators, as shown in Figure 2. The top end of the prismatic joints consists of magnetic solenoids (a1 & a2) with an adhesive force of 147 N. Similarly, the bottom of both prismatic joints is connected with another two magnetic solenoids (b1 & b2) with an adhesive force of 147 N, which is fed as input in the Lua script.

The two prismatic joints (linear actuators) are coupled with a central electromagnetic disc having three solenoids, Sc, Sd, Se, with a magnetic adhesive force value of 343 N from each solenoid. Hence, the total adhesive force of 1029 N (343 x 3) will be fed as input to the simulation through a Lua script. This 1029 N adhesive force exerted from the central disc will be activated only in static mode, particularly when the H-Bot needs to change the direction of its movement.

The vertical metal wall environment is created in the Coppelia Sim software, as shown in Figure 2. The designed H-Bot is allowed to climb a distance of 100 cm, and the respective time taken is noted as shown in Table 4. Similarly, the H-Bot is allowed to descend, and the time taken to reach the starting point is noted and tabulated as shown in Table 5. The time taken value in the simulation will be compared with that of the actual time taken for the fabricated hardware H-bot during the lab test.

Fig. 2 Simulation of H-Bot in CoppeliaSim

3. Mathematical Modeling

The mathematical model for the proposed design H-Bot is obtained via a free-body diagram. The Figure 3 to Figure 6 shows the proposed bot in various position like on the horizontal surface for case A, on the inclined surface for case B, on the vertical surface for case C and upside down inverted on the surface for case D.

The required adhesive force for each case is discussed in detail through free body diagram leading to derive a mathematical equation via which the adhesive force is obtained. The desired adhesive force obtained in each case is tabulated in Table 2.

Case A: Considering the weight of the bot as $W_{G,}$ and the H-bot is considered to be resting on the horizontal surface. The desired adhesive force in this case is denoted as $f^{l}_{a.}$ There are four solenoids (a1, a2,b1,b2) in touch with the surface; the adhesive force exerted from that electromagnetic solenoid is denoted as S_{a1}, $S_{a2,}$ and S_{b1}, S_{b2}. Since the adhesive force exerted from the solenoids in the central electromagnetic disc (S_c, $S_{d,}$ and S_e) is not in touch with the surface and not in active mode during the movement, it is not considered for calculation. These S_c, $S_{d,}$ and S_e are active only when there is a change in direction. The desired adhesive for the H-Bot in this case is as given in equation 1.

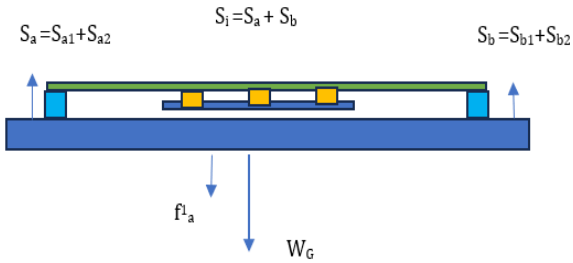

Fig. 3 The H-Bot on a horizontal surface

$$\sum_{i=0}^{i=2} Sai + \sum_{i=0}^{i=2} Sbi = WG + f1a \quad (1)$$

Case B: Considering the weight of the bot as $W_{G,}$ and the H-bot is considered to be climbing on the inclined surface, having $\boldsymbol{\theta}$ as the angle of inclination. The desired adhesive force in this case is denoted as $f^{2}_{a.}$ There are four solenoids (a1, a2,b1,b2) in touch with the surface; the adhesive force exerted from that electromagnetic solenoid is denoted as S_{a1}, $S_{a2,}$ and S_{b1}, S_{b2}.

Since the adhesive force exerted from the solenoids in the central electromagnetic disc (S_c, $S_{d,}$ and S_e) is not in touch with the surface and not in active mode during the movement, it is not considered for calculation. These S_c, $S_{d,}$ and S_e are active only for a change in direction. The desired adhesive for the H-Bot in this case is as given in equation 2.

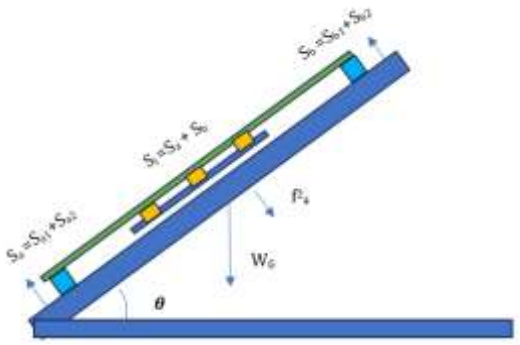

Fig. 4 The H-Bot on an inclined surface

$$\sum_{i=0}^{i=2} Sai + \sum_{i=0}^{i=2} Sbi = WGCos\Theta + f2a \quad (2)$$

Case C: Considering the weight of the bot as W_G, and the H-bot is considered to be climbing on the vertical surface, having $\boldsymbol{\theta}$ as the perpendicular to the ground surface. The desired adhesive force in this case is denoted as f^3_a. There are four solenoids (a1, a2, b1,b2) in touch with the surface; the adhesive force exerted from that electromagnetic solenoid is denoted as S_{a1}, S_{a2}, and S_{b1}, S_{b2}. Since the adhesive force exerted by the solenoids in the central electromagnetic disc (S_c, S_d, and S_e) is not in touch with the surface and not in active mode during the movement, it is not considered for calculation. These S_c, S_d, and S_e are active only for a change in direction. The desired adhesive for the H-Bot in this case is as given in equation 3.

$$\sum_{i=0}^{i=2} Sai + \sum_{i=0}^{i=2} Sbi = f3a \quad (3)$$

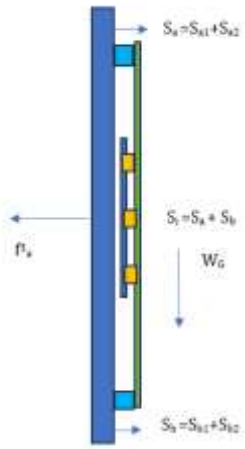

Fig. 5 The H-Bot on a vertical surface

Case D: Considering the weight of the bot as W_G, the H-bot is considered to be climbing on the upside-down inverted surface. The desired adhesive force in this case is denoted as f^4_a. There are four solenoids (a1, a2,b1,b2) in touch with the surface; the adhesive force exerted from that electromagnetic solenoid is denoted as S_{a1}, S_{a2}, and S_{b1}, S_{b2}. Since the adhesive force exerted from the solenoids in the central electromagnetic disc (S_c, S_d, and S_e) is not in touch with the surface and not in active mode during the movement, it is not considered for calculation. These S_c, S_d, and S_e are active only for a change in direction. The desired adhesive for the H-Bot in this case is as given in equation 4.

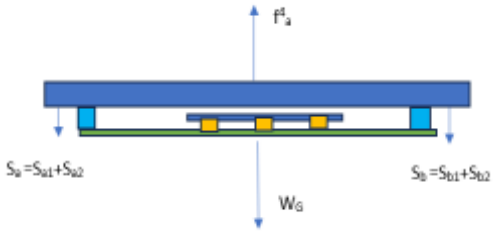

Fig. 6 The H-Bot in upside-down inverted position

$$\sum_{i=0}^{i=2} Sai + \sum_{i=0}^{i=2} Sbi + WG = f4a \quad (4)$$

Table 2. Desired adhesive force in each case

CaseA	Case B	Case C	Case D
538 N	567 N	588 N	618 N

Considering the desired adhesive force during dynamic mode required for each case as given in the table, the actual proposed H-bot is designed with 588 N, as it is about to climb the vertical wall. The adhesive force of each central electromagnet or solenoid is 343 N, and since there are three solenoids (ie, Sc, Sd, Se), the total adhesive force exerted from the central disc when it is touching the surface will be (343 x 3=1029N), which is far enough to lift the overall weight during the static mode for changing the direction. This 1029N adhesive force exerted from the central disc gives high stability during direction change, which is not present in other existing research.

4. FEMM Simulation

The proposed H-Bot is modelled in 2D geometry, and the materials are assigned. In FEMM, the boundary conditions need to be provided, and use finite-element techniques to run a solver. The proposed model of H-bot is designed in FEMM software in order to study the flow of magnetic flux lines throughout the length of the H-bot, as shown in Figure 7. This analysis also picturizes the level of magnetic field intensity exerted along the dimension of the WCR. The strength of magnetic flux ranges between 1.86 e^0 and 1.96 e^0. The contour is declared along the length of both linear actuators as shown in Figures 8 and 9. Analyzing Figures 10 to 23, it is observed that a uniform pattern of graph is obtained for both the linear actuators l1 and l2 (justifying the design of the proposed H-

bot) under various cases like potential, H-field, peripheral field intensity, tangential flux strength, normal field intensity, normal H-density, and magnitude of field intensity. It seems that magnetic flux density and magnitude of field intensity, tangential field strength and flux strength, normal field intensity and flux density are uniformly distributed along the length of the H-Bot.

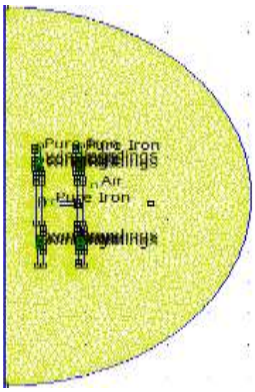

Fig. 7 The H-Bot design & analysis with mesh created in FEMM

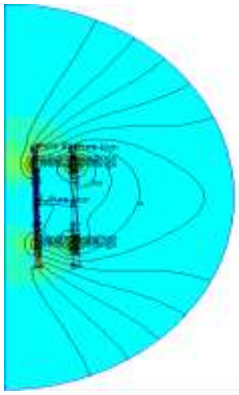

Fig. 8 The H-Bot design & analysis with flux lines in FEMM

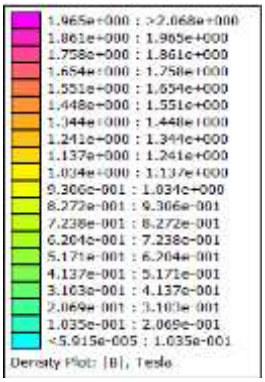

Fig. 9 The H-Bot design & analysis scale of magnetic flux in FEMM

The switching of the solenoids follows some pattern in such a way that hopping is done efficiently while climbing up or down on the wall. Table 3 explains the switching mode of solenoids when the H-bot is in ascending motion, descending motion, and while changing direction (360-degree rotation). The green color indicates that those solenoids were in active energized, and the orange color indicates that those solenoids were DE energized for that particular mode of operation.

Table 3 explains the switching mode of solenoids when the H-bot is in ascending motion, descending motion, and also while changing direction (360-degree rotation). The entire methodology hence starts with mathematical modelling, FEMM software for magnetic flux lines, Coppeliasim software for modelling and design, and final real-time fabrication and testing in both static and dynamic modes.

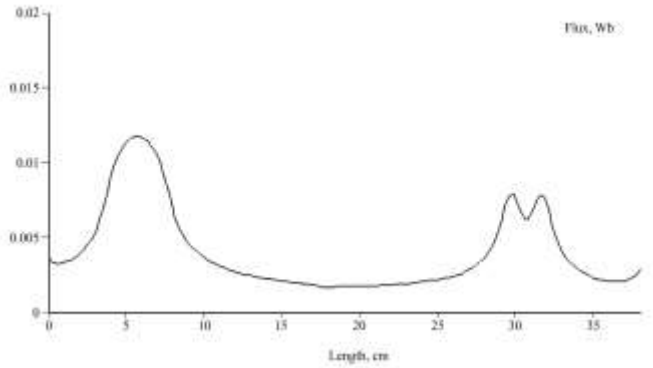

Fig. 10 Potential in l1

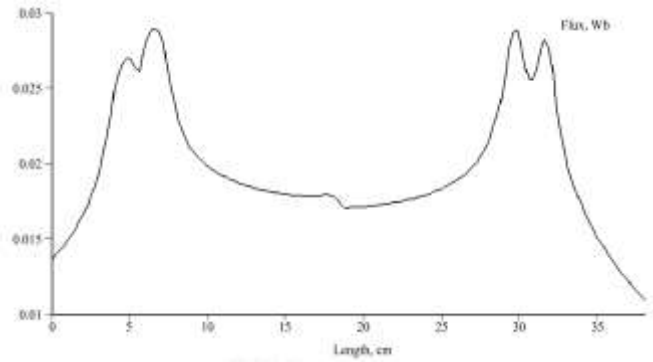

Fig. 11 Potential in l2

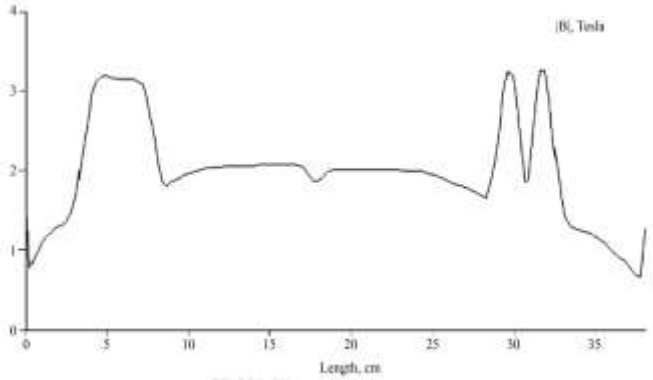

Fig. 12 Magnitude of flux density in l1

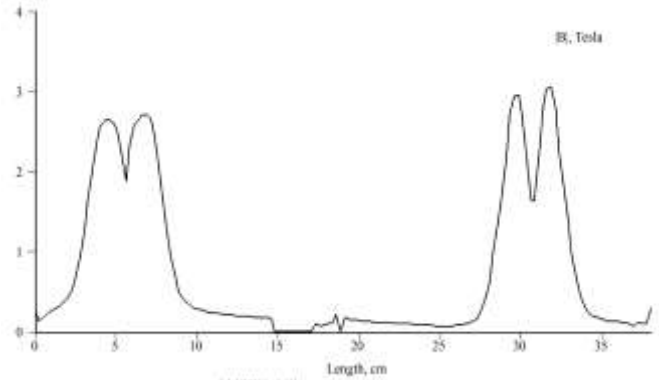

Fig. 13 Magnitude of flux density in l2

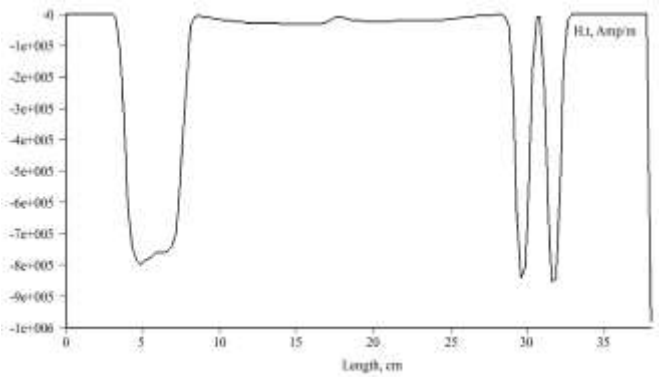

Fig. 14 Tangential field intensity in l1

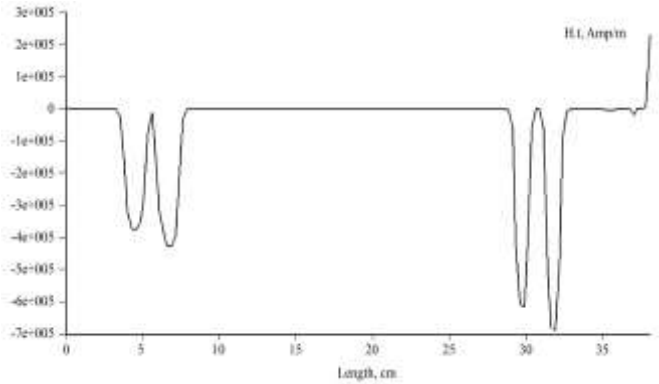

Fig. 15 Tangential field intensity in l2

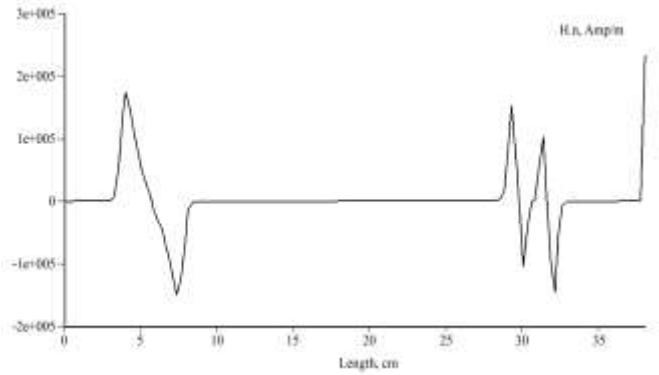

Fig. 16 Tangential flux density in l1

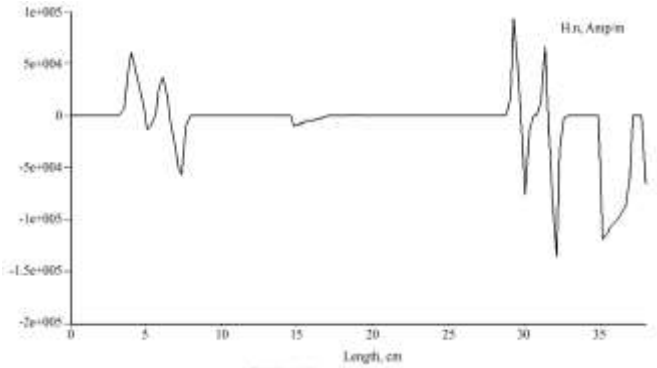

Fig. 17 Tangential flux density in l2

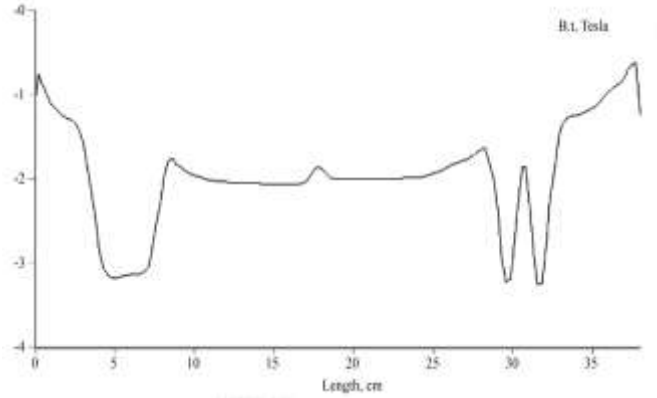

Fig. 18 Normal field intensity in l1

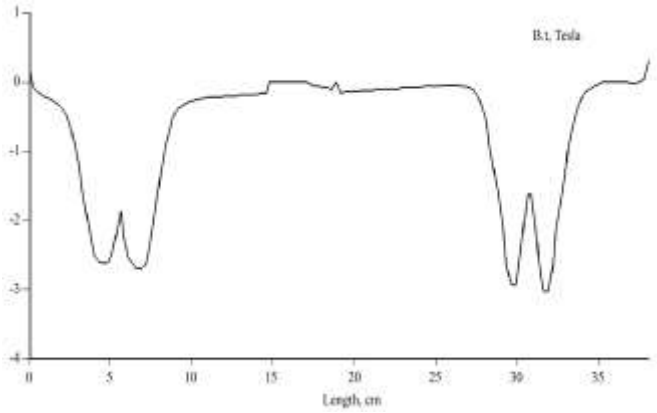

Fig. 19 Normal field intensity in l2

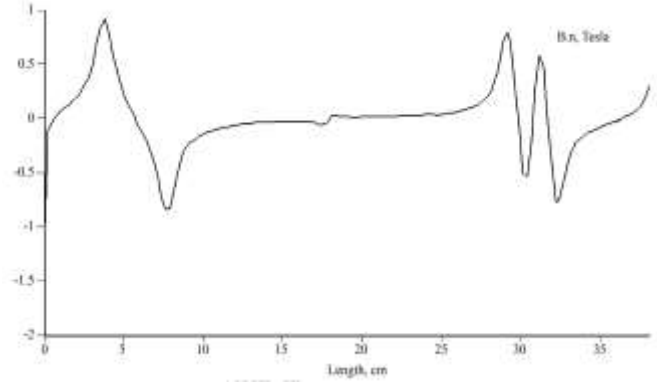

Fig. 20 Normal flux density in l1

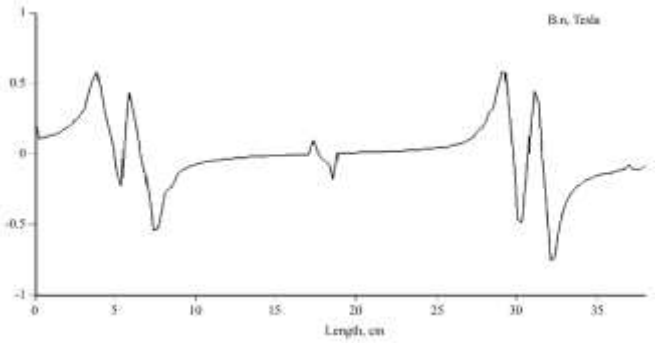

Fig. 21 Normal flux density l2

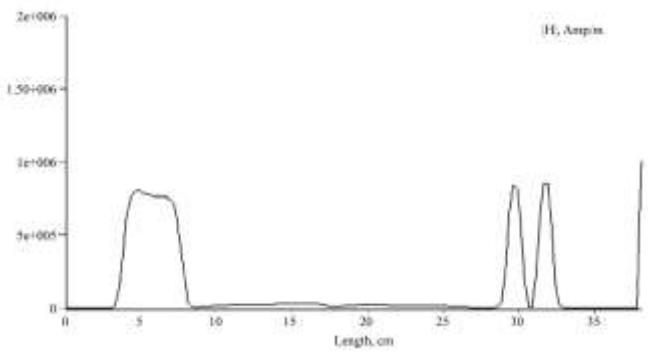

Fig. 22 Magnitude of field intensity in l1

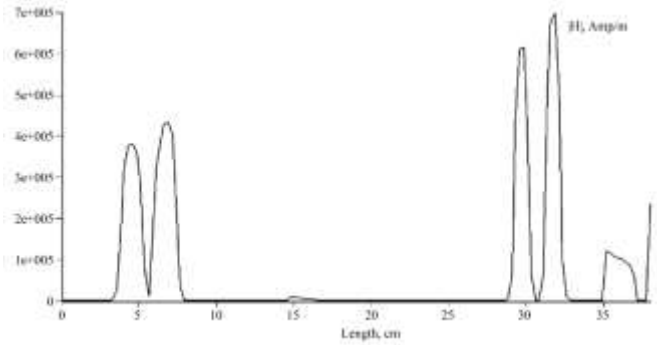

Fig. 23 Magnitude of field intensity in l2

Fig. 24 H-Bot in 90^0

Fig. 25 H-Bot in 60^0

Fig. 26 H-Bot in 30^o

Fig. 27 H-Bot in 0^o

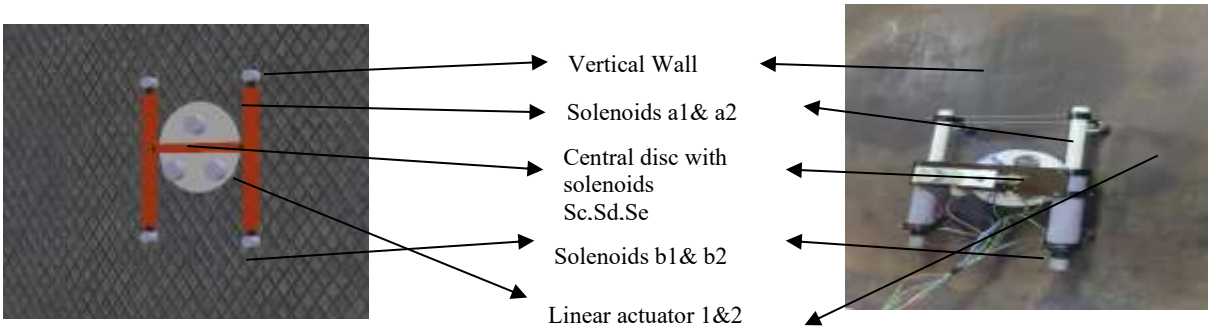

Fig. 28 Parts of the H-Bot in software test

Fig. 29 Parts of the H-Bot in hardware test

Table 3. Switching mode of solenoids

Solenoid energizing	Sa1	Sa2	Sb1	Sb2	Sc	Sd	Se
	H-Bot in Forward Movement						
Step1							
Step2							
	H-Bot in Reverse Movement						
Step1							
Step2							
	H-Bot in Omni Direction mode						
Step1							

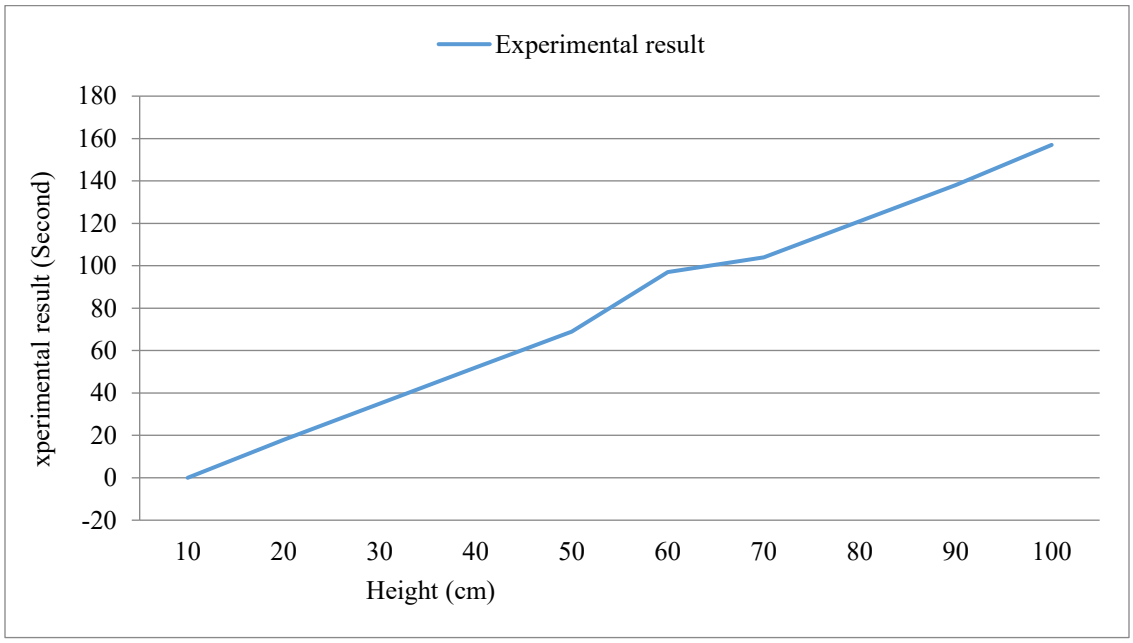

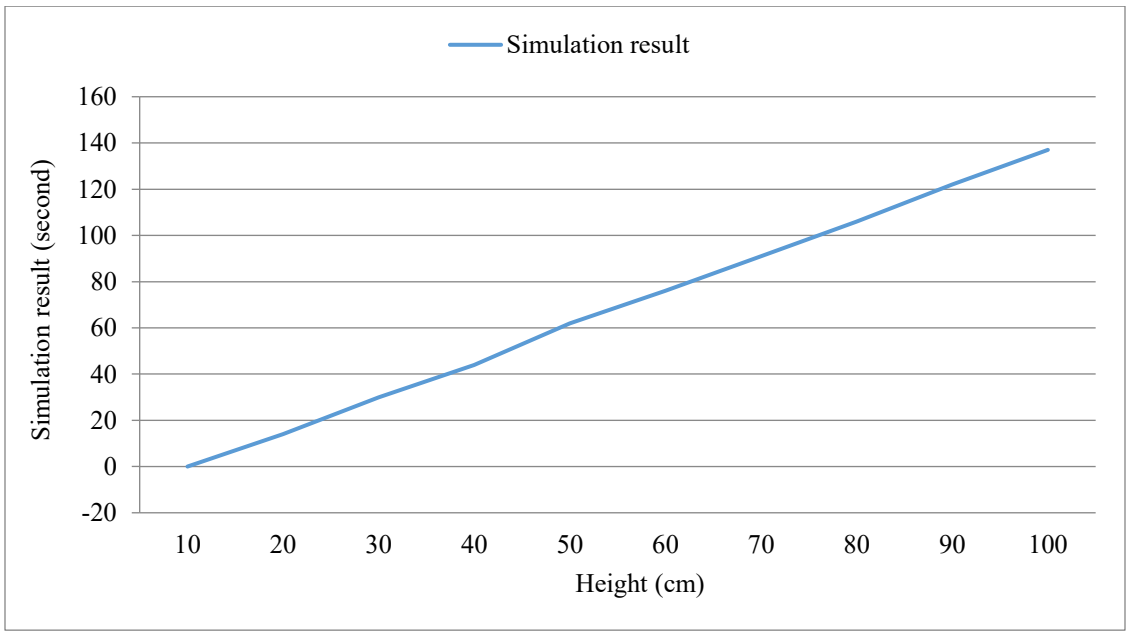

Fig. 30 Simulation Vs Experimental-H-Bot ascending

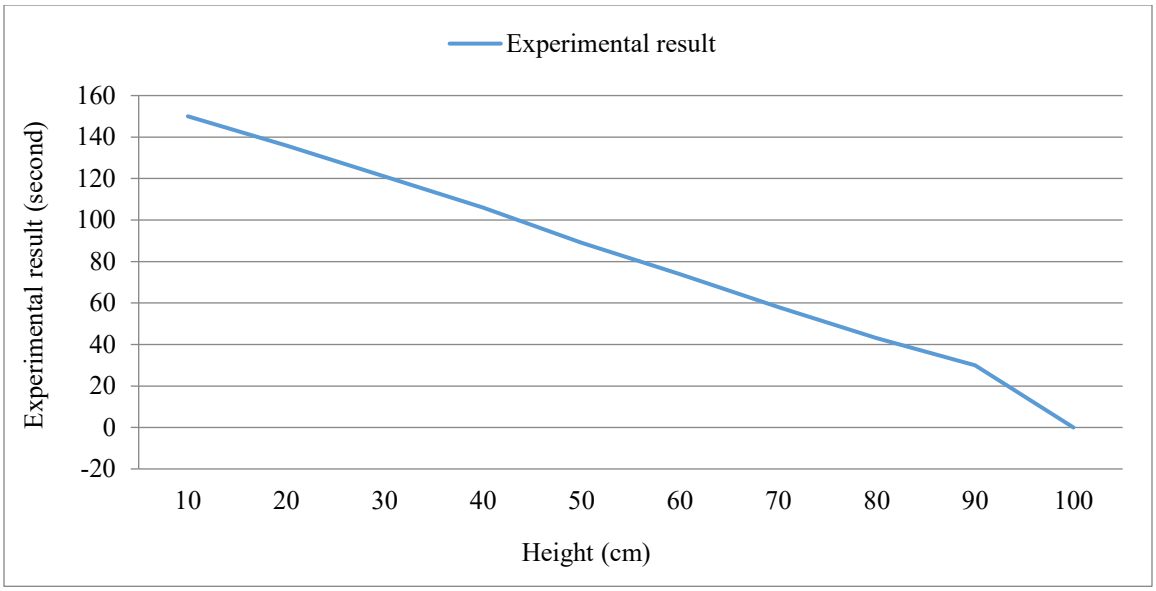

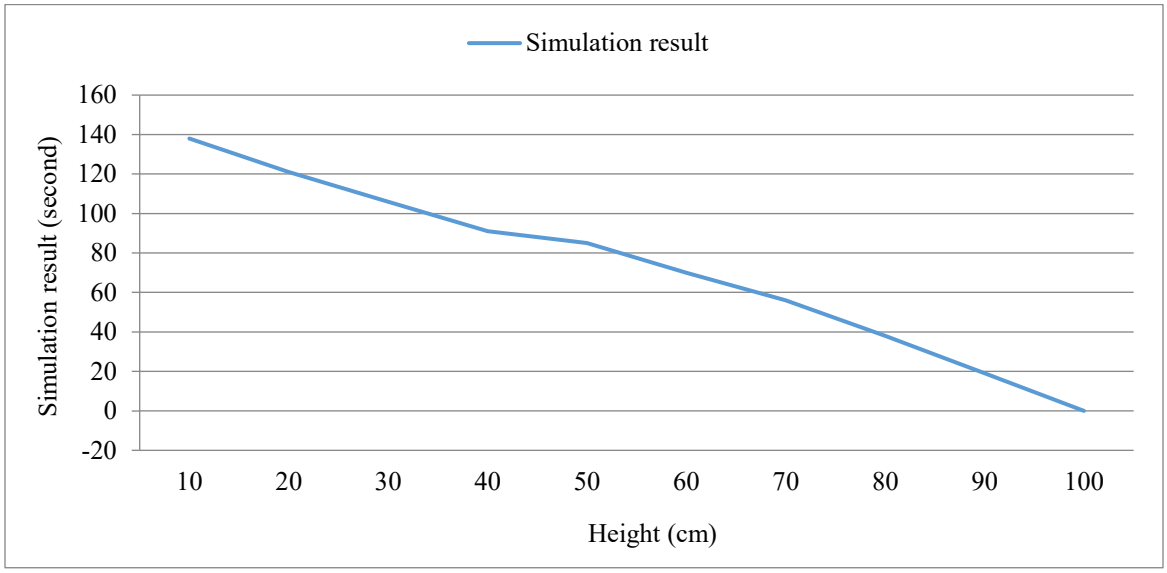

Fig. 31 Simulation Vs Experimental -H-bot descending

Table 4. H-Bot ascending the wall

Simulation Vs Exp result		
	Simulation Result	**Exp Result**
Height	**Time**	**Time**
cm	seconds	seconds
10	0	0
20	14	18
30	30	35
40	44	52
50	62	69
60	76	97
70	91	104
80	106	121
90	122	138
100	137	157

Table 5. H-Bot descending the wall

Simulation Vs Exp result		
	Simulation Result	Exp Result
Height	Time	Time
cm	seconds	seconds
100	0	0
90	19	30
80	38	43
70	56	58
60	70	74
50	85	89
40	91	106
30	106	121
20	121	136
10	138	150

5. Result and Discussion

Figures 24 to 27 show the angle of rotation proving the omni direction rotation of the real-time fabricated H-Bot on the vertical wall. Figure 28 is the simulation model of the proposed H-Bot, and Figure 29 is the real-time fabricated H-Bot. Figure 30 shows that the time taken by the H-Bot while ascending to reach a particular height is the same in both simulation and real-time hardware testing. The time taken Vs height reach data for H-Bot ascending is shown in Table 4. The average ascending time obtained experimentally is 0.57 cm/s compared to 0.66cm/s obtained through simulation. The mean absolute error obtained is 12.1s, and the quadratic mean error is 13.9s; the Pearson correlation coefficient is 0.997. Figure 31 shows that the time taken by H-Bot while descending to reach a particular height, both in the case of simulation and real-time hardware testing, is almost the same. The time taken Vs height reach data for H-Bot descending is shown in Table 5. The average descending time obtained experimentally is 0.60 cm/s compared to 0.65cm/s obtained through simulation. The mean absolute error obtained is 9.22s, and the quadratic mean error is 10.9s; the Pearson correlation coefficient is 0.998.

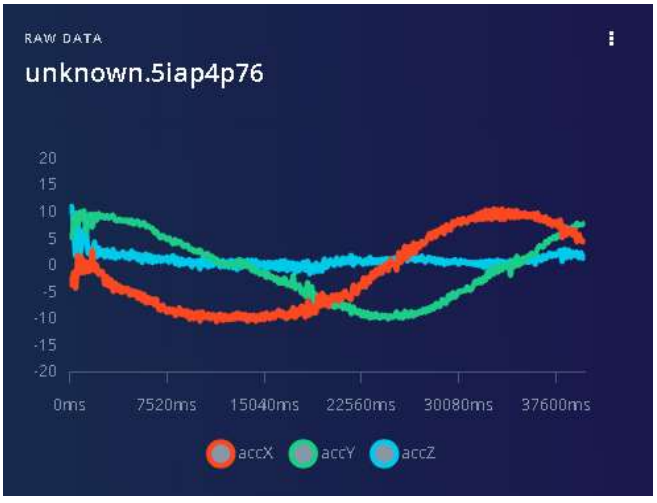

Fig. 32 Stability analysis in clockwise rotation via Edge impulse

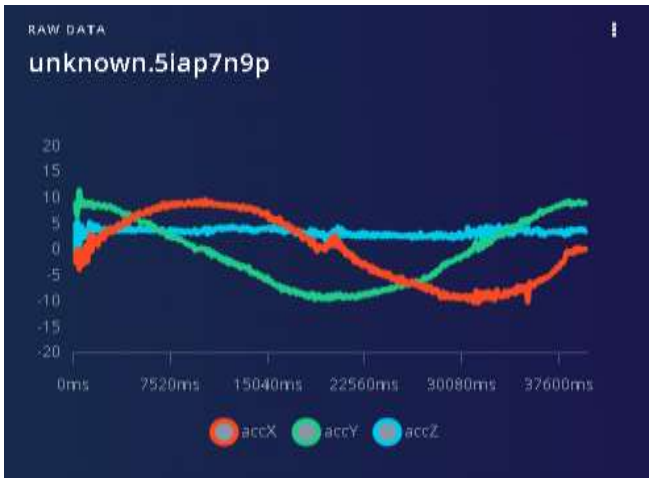

Fig. 33 Stability analysis in anticlockwise rotation via Edge impulse

The accelerometer and gyroscope sensor fixed on the H-Bot is linked with Edge impulse software to have live continuous monitoring over the position of the H-Bot in a dynamic state, either while climbing or ascending the wall, or while descending or getting down on the vertical metal wall.

Figure 32 shows the stability analysis of H-Bot in clockwise rotation via Edge Impulse software. Figure 33 shows the stability analysis of H-Bot in anticlockwise rotation. While analyzing Figures 32 and 33, there is less deviation in the z-axis, which means the H-Bot is stable in its position, and the variation in the x and y axes is found to be in harmony both during clockwise and anticlockwise rotation, which means the H-Bot is stable while rotating.

6. Conclusion

The mathematical model for the proposed H-Bot design has enhanced the software modeling in Coppelia Sim. The graph obtained using FEMM analysis of the proposed design has also justified the capability of the proposed model under various categories, as shown in Figures 10 to 23. The time

taken with respect to the height reached, both in the case of simulation and real-time hardware testing, is found to be the same, which shows that CoppeliaSim can be a vital and active mode for modelling and design of WCR.

This reduces the unnecessary scrap cost that happens through the traditional trial-and-error method while fabricating the robot. The stability graph along the x-axis, y-axis, and z-axis obtained via Edge impulse software is obtained by coupling the H-bot hardware through IoT to the Edge impulse software.

While analyzing Figures 32 and 33, it is obvious to understand the fact that there is no deviation in z-axis value and a harmonical positive Sine wave obtained for anticlockwise rotation and a harmonical Negative Sine wave obtained for clockwise rotation of the H-bot indicates that omni direction rotation is successfully enhanced in this proposed H-bot wall climbing Robot. This H-Bot can be further tested in a real-time environment or an industrial application as a part of future work, as it may include other environmental factors that may influence the design, as the current one has been merely tested in a lab environment.

Acknowledgement

Need to acknowledge the open source platform named Edge Impulse software, which acted as a platform to do this project, and also need to thank the Coppelia Sim software for enhancing the simulation modelling and validation of the H-bot WCR. The lab test done with the fabricated hardware module has neglected certain industrial environmental parameters.

Though the proposed design of H-bot can overcome small discontinuities in the wall surface (which cannot be done in a wheeled-type wall climbing robot), it cannot overcome obstacles on the surface. The lab test was performed in the Robotics lab, established at PMIST, with high industrial safety standards.

References

[1] Omar Faruq Howlader, and Traiq Pervez Sattar, "Finite Element Analysis based Optimization of Magnetic Adhesion Module for Concrete Wall Climbing Robot," *International Journal of Advanced Computer Science and Applications*, vol. 6, no. 8, pp. 8-18, 2015. [CrossRef] [Google Scholar] [Publisher Link]

[2] Love P. Kalra, Jason Gu, and Max Meng, "A Wall Climbing Robot for Oil Tank Inspection," *2006 IEEE International Conference on Robotics and Biomimetics*, Kunming, China, pp. 1523-1528, 2006. [CrossRef] [Google Scholar] [Publisher Link]

[3] Giuk Lee et al., "Compliant Track-Wheeled Climbing Robot with Transitioning Ability and High-Payload Capacity," *2011 IEEE International Conference on Robotics and Biomimetics*, Karon Beach, Thailand, pp. 2020-2024, 2011. [CrossRef] [Google Scholar] [Publisher Link]

[4] Haocai Huang et al., "Design and Performance Analysis of a Tracked Wall-Climbing Robot for Ship Inspection in Shipbuilding," *Ocean Engineering*, vol. 131, pp. 224-230, 2017. [CrossRef] [Google Scholar] [Publisher Link]

[5] Baoyu Wang et al., "Development of a Wheeled Wall-Climbing Robot with an Internal Corner Wall Adaptive Magnetic Adhesion Mechanism," *Journal of Field Robotics*, vol. 42, no. 1, pp. 97-114, 2025. [CrossRef] [Google Scholar] [Publisher Link]

[6] Ze Jiang et al., "Design and Analysis of a Wall-Climbing Robot for Water Wall Inspection of Thermal Power Plants," *Journal of Field Robotics*, vol. 40, no. 5, pp. 1003-1013, 2023. [CrossRef] [Google Scholar] [Publisher Link]

[7] Xiaosong Li et al., "Robust Scalable Reversible Strong Adhesion by Gecko-inspired Composite Design," *Friction*, vol. 10, pp. 1192-1207, 2022. [CrossRef] [Google Scholar] [Publisher Link]

[8] Zhen Qian, and Hanbiao Xia, "Study of a Wall-Climbing Robot based on Chain feet with Negative Pressure Adhesion," *Discover Applied Sciences*, vol. 6, pp. 1-16, 2024. [CrossRef] [Google Scholar] [Publisher Link]

[9] Pei Yang et al., "A Lightweight Optimal Design Method for Magnetic Adhesion Module of Wall-Climbing Robot based on Surrogate Model and DBO Algorithm," *Journal of Mechanical Science and Technology*, vol. 38, 2041-2053, 2024. [CrossRef] [Google Scholar] [Publisher Link]

[10] Gang Wang, Wenjun Li, and Honglei Che, "Design and Analysis of Anti-Overturning Mechanism for Magnetic Wall-Climbing Robot," *Journal of Mechanical Science and Technology*, vol. 38, pp. 379-387, 2024. [CrossRef] [Google Scholar] [Publisher Link]

[11] Junru Zhu, Yongqiang Zhu, and Pingxia Zhang, "Review of Advancements in Wall Climbing Robot Techniques," *Franklin Open*, vol. 8, pp. 1-20, 2024. [CrossRef] [Google Scholar] [Publisher Link]

[12] Shanqiang Wu et al., "A Magnetic Wall Climbing Robot with Non-Contactable and Adjustable Adhesion Mechanism," *2017 IEEE International Conference on Real-time Computing and Robotics (RCAR)*, Okinawa, Japan, pp. 427-430, 2017. [CrossRef] [Google Scholar] [Publisher Link]

[13] Ajmal Khan, Wasim Ahmad, and Salman Hussain, "Design and Fabrication of Wall-Climbing Robot Using Magnetic Adhesion," *Engineering Proceedings*, vol. 111, no. 1, pp. 1-11, 2025. [CrossRef] [Google Scholar] [Publisher Link]

[14] Hao Xu et al., "NuBot: A Magnetic Adhesion Robot with Passive Suspension to Inspect the Steel Lining," *Chinese Journal of Mechanical Engineering*, vol. 36, pp. 1-18, 2023. [CrossRef] [Google Scholar] [Publisher Link]

[15] Junyu Hu et al., "A Magnetic Crawler Wall-Climbing Robot with Capacity of High Payload on the Convex Surface," *Robotics and Autonomous Systems*, vol. 148, 2022. [CrossRef] [Google Scholar] [Publisher Link]

[16] Stefan Leuthard et al., "Magnecko: Design and Control of a Quadrupedal Magnetic Climbing Robot," *Walking Robots into Real World: Proceedings of the CLAWAR 2024 Conference*, vol. 2, pp. 55-67, 2025. [CrossRef] [Google Scholar] [Publisher Link]

[17] Rakesh Rajendran et al., "Design of Omnidirectional Wall Climbing Robot with Its Payload Analysis" *International Research Journal of Multidisciplinary Scope (IRJMS)*, vol. 6, no. 2, pp. 1112-1120, 2025. [CrossRef] [Publisher Link]